

Adjoint Stability and Miss Distance in Proportional Navigation

Orly Goldan*

Israel Aircraft Industries, Ltd., 70350 Beer Yaakov, Israel

and

Shaul Gutman†

Technion–Israel Institute of Technology, 32000 Haifa, Israel

DOI: 10.2514/1.56143

In this paper, the performances of bounded evasive maneuvers against a missile guided by proportional navigation (PN) are considered. Naturally, guidance systems operate on a finite time interval, and the miss distance is measured at the end of this interval. Can a rational evasive maneuver force an increasing miss with an increasing time interval? A positive answer implies that an evasive target may force unbounded miss distance by starting the maneuver early enough. Taking the time interval to infinity, the connection of bounded miss distance in PN with asymptotic stability of the adjoint system is shown. Although this is clear on an intuitive level, it is important to present a rigorous proof and the correspondent conditions. In particular, under mild conditions, the worst miss is bounded over the infinite flight time.

I. Introduction

PROPORTIONAL navigation (PN) has a successful 60 year history despite its simplicity [1–4]. In PN the command acceleration normal to the line of sight (LOS) is proportional to the LOS rate. Under the assumption of a small deviation normal to the LOS, its linear mathematical model consists of a feedback loop having a double integrator with a time varying gain as the kinematics, and the missile transfer function as dynamics. The gain, inverse of the time to go, spans from zero far away from termination to infinity at termination. While many quantitative results concerning PN exist [1], very little has been done qualitatively. Exceptional is [5–7] where finite time stability is discussed. In finite time stability we mean that some distance in the sense of a positive definite quadratic form in the state space decreases with time. It turns out that sufficiently close to termination finite time stability is not guaranteed. In fact, if the miss distance is sufficiently small and nonzero, the LOS rate tends to infinity, so that any such a quadratic form diverges before termination. It is stressed that although the LOS rate tends to infinity, the miss distance stays finite. This suggests that with regard to PN, the notion of finite time stability should be reexamined. In the present Note, miss distance and stability are connected, but unlike [5], the stability of the adjoint system is studied. The reason is twofold. First, while the PN forward simulation generates the miss distance for a specific time to go, a single adjoint simulation generates the miss distance for all time to go. Second, the miss distance has a special connection with the adjoint system. In particular, the worst miss distance induced by an arbitrary bounded evasive maneuver is proportional to the time integral absolute value of a certain state of the adjoint loop [8]. Thus, exponential stability is required for the infinite time integral to converge. Put it differently, if the adjoint asymptotic stability is not assured, a bounded evasive maneuver may force an arbitrary large miss distance by starting the maneuver early enough. It is shown here that under mild conditions, the adjoint system is exponentially stable, and consequently, the worst miss is bounded over the infinite flight time.

II. System Models

Consider a conflict of two objects, a missile M and a target T , moving in a plane. Basically, the kinematics of these objects is nonlinear. However, it is a common practice to linearize the preceding motion perpendicular to the LOS. To this end, consider the nominal collision triangle, in which M and T move in constant speeds and directions toward a collision point C . We assume that along the nominal LOS the closing speed $V_c = -\dot{R}$ is positive and approximately constant. In the direction normal to the LOS the target maneuvers with a lateral acceleration v , and the missile with a lateral acceleration u . In this conflict we assume that the missile uses the classical linear strategy PN, while the target uses a bounded maneuver v so as to maximize the miss distance. To extract the mathematical model, consider Fig. 1 in which V_M and V_T are the corresponding velocity vectors (having constant magnitudes), and where the approximation is done normal to the initial LOS. We define the time to go by $t_{go} := t_f - t$, where t_f is the final time, and it is assumed that along the LOS, the range R satisfies the nominal relation

$$R = (V_M \cos \phi_M - V_T \cos \phi_T) t_{go} := V_c t_{go}$$

Figure 2 describes the kinematics of the engagement and the missile dynamics, where $x_1 := y_T - y_M := \Delta y$ is the separation of the two objects normal to the LOS, $x_2 := \Delta \dot{y}$, and the dynamics of the missile is described either by its transfer function or by its realization according to

$$\frac{u(s)}{u_c(s)} := G_M(s): \begin{cases} \dot{z} = \hat{A}z + \hat{b}u_c \\ u = \hat{c}z + \hat{d}u_c \end{cases} \quad (1)$$

Let $x := [x_1 \quad x_2 \quad z']^T$. Assuming an ideal target, we obtain the linear model:

$$\dot{x} = Ax + Bu_c + Cv \quad (2)$$

where

$$A = \begin{bmatrix} 0 & 1 & 0 \\ 0 & 0 & -\hat{c} \\ 0 & 0 & \hat{A} \end{bmatrix}, \quad B = \begin{bmatrix} 0 \\ -\hat{d} \\ \hat{b} \end{bmatrix}, \quad C = \begin{bmatrix} 0 \\ 1 \\ 0 \end{bmatrix}$$

In this Note we apply PN, in which the missile's command lateral acceleration u_c is proportional to the LOS rate:

$$u_c = N' V_c \dot{\sigma} \quad (3)$$

Presented as Paper 2011-6417 at the AIAA Guidance, Navigation, and Control Conference, Portland, OR, 8–11 August 2011; received 15 September 2011; revision received 13 December 2011; accepted for publication 13 December 2011. Copyright © 2011 by the American Institute of Aeronautics and Astronautics, Inc. All rights reserved. Copies of this paper may be made for personal or internal use, on condition that the copier pay the \$10.00 per-copy fee to the Copyright Clearance Center, Inc., 222 Rosewood Drive, Danvers, MA 01923; include the code 0731-5090/12 and \$10.00 in correspondence with the CCC.

*Systems Missiles and Space Group, MLM Division.

†Department of Mechanical Engineering.

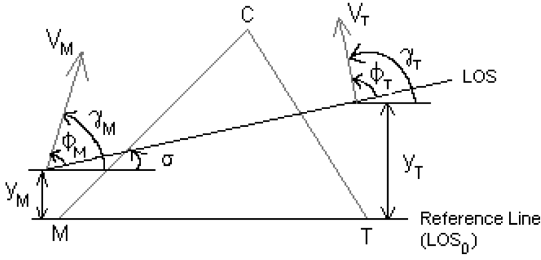


Fig. 1 Collision triangle and perturbations.

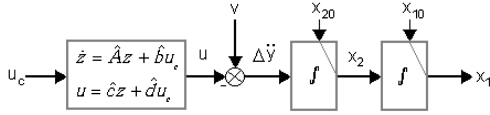


Fig. 2 Open loop block diagram.

where N' is the navigation gain, and σ is the LOS orientation in an inertial frame, and is defined by $\sigma = x_1/V_c t_{go}$. Applying this guidance law one can draw the closed loop block diagram presented in Fig. 3a. Notice that this realization contains a differentiator. To be able to present the guidance equations in state space (for purposes such as optimal control analysis), we take the derivative according to

$$\sigma = \frac{x_1}{V_c t_{go}} \Rightarrow t_{go}^2 V_c \dot{\sigma} = x_1 + t_{go} x_2 \quad (4)$$

and present the corresponding block diagram in Fig. 3b. Another simplification of Fig. 3b can be made by using the fact that

$$\frac{d}{dt}(x_1 + t_{go} x_2) = t_{go} \dot{x}_2 \quad (5)$$

and implementing it Fig. 3d. In this case the output should be integrated twice in order to get the miss distance. Note that Figs. 3a, 3b, and 3d are equivalent. For the important special case, where N' is constant, Fig. 3c represents a simplified version of Fig. 3a. In all these diagrams the only input is a bounded target maneuver, which is considered to be an unknown deterministic function. In the present Note we will neglect the influence of measurements noise. Thus the assumption of a constant V_c makes it possible to cancel out V_c from the miss distance calculation in the block diagrams.

III. Worst Miss Distance

In this section we seek the worst miss distance, under the assumption that the target maneuver is an arbitrary bounded function.

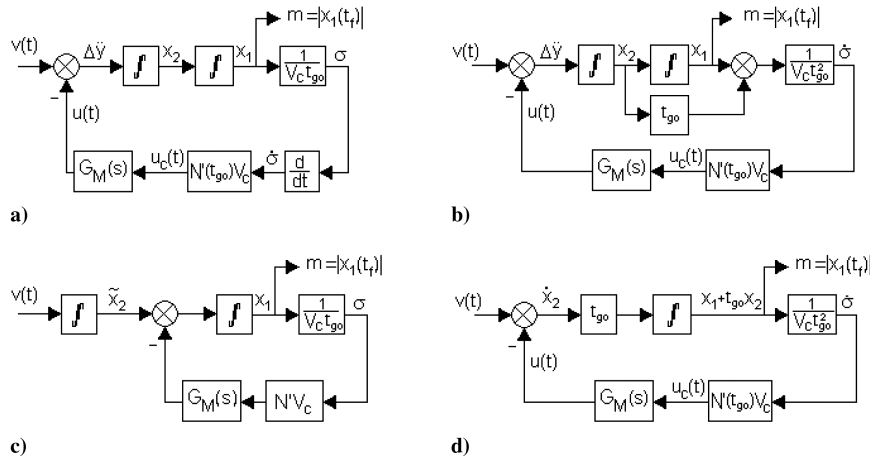


Fig. 3 Proportional navigation block diagrams.

The worst miss distance and its corresponding target maneuver will be found using the adjoint system technique. While the classical adjoint approach to miss distance deals with a step target maneuver [1], we show that the extension to the worst bounded target maneuver is straight forward. Let $g(t, \tau)$ be the response of a linear system at time t to an impulse at time τ . Let $f(t_f - \tau, t_f - t)$ be the response of the adjoint system at $t_f - \tau$ to an impulse at $t_f - t$. Then, $f(t_f - \tau, t_f - t) = g(t, \tau)$; see [9]. As a result, at time t_f , $f(t_f - \tau, 0) = g(t_f, \tau)$. However, using convolution, we have the response

$$y(t_f) = \int_0^{t_f} g(t_f, \tau) v(\tau) d\tau \quad (6)$$

since $|v(t)| \leq \rho_v$, it follows now that

$$\begin{aligned} |y(t_f)| &\leq \int_0^{t_f} |g(t_f, \tau) v(\tau)| d\tau \leq \rho_v \int_0^{t_f} |g(t_f, \tau)| d\tau \\ &= \rho_v \int_0^{t_f} |f(t_f - \tau, 0)| d\tau = \rho_v \int_0^{t_f} |f(\eta, 0)| d\eta \\ &:= \rho_v \int_0^{t_f} |f(\eta)| d\eta \end{aligned}$$

where $\eta = t_f - \tau$ plays the role of t_{go} . Finally,

$$|y(t_f)| \leq m(t_{go}) := \rho_v \int_0^{t_{go}} |f(\eta)| d\eta \quad (7)$$

and the worst miss distance [8] is

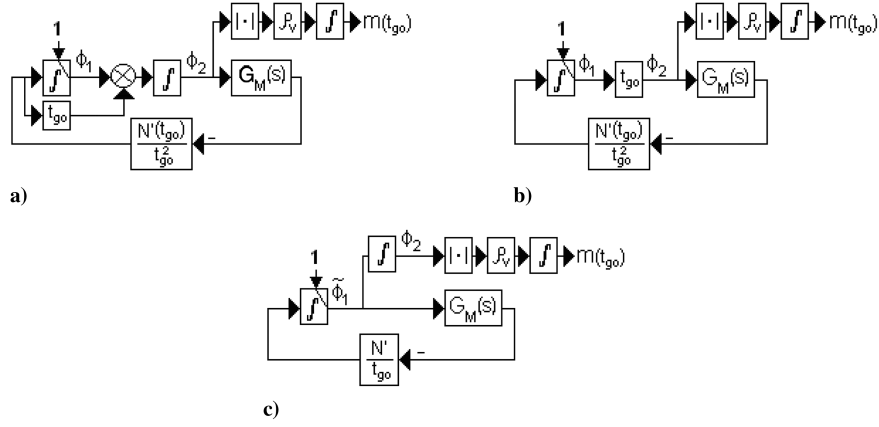
$$m^* := \rho_v \int_0^\infty |f(t_{go})| dt_{go} \quad (8)$$

Note that in the series of the inequalities, the target maneuver v^* , that generates the upper bound, satisfies

$$v^*(t) = \pm \rho_v \text{sgn}[f(t_{go})] \quad (9)$$

To see this result, recall that $\max_{|v| \leq \rho_v} |g(t_f, \tau) v(\tau)| = \rho_v |g(t_f, \tau)|$ and that it is attained at $v^*(\tau) = \pm \rho_v \text{sgn}[g(t_f, \tau)]$.

The diagrams in Figs. 4a–4c are the adjoints of the systems described in Figs. 3b–3d, respectively. Indicating the output of each adjoint as $f(t_{go}) := \phi_2(t_{go})$, m^* is the steady-state value of $m(t_{go})$ in Figs. 4a–4c. Also, since for a constant N' all of the guidance loops of Fig. 3 are the same, m^* and $\phi_2(t_{go})$ are equal in all the implementations of Fig. 4. Unlike [8], chap. 9, where a special case of the differential game approach is used, here a classical adjoint approach is taken. A typical function of $m(t_{go})$ is illustrated in Fig. 5 for $G_M(s)$ of first order. As a reference function we have composed a dashed line that represents the sensitivity function $m(t_{go})$ for a step target maneuver.

Fig. 4 Block diagrams for $m(t_{go})$.

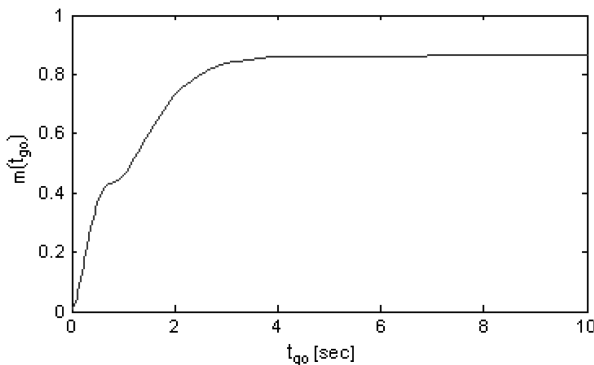
IV. Adjoint System Stability

Guidance systems operate on a finite time interval. Hence, for some specific flight time t_{go} , the corresponding miss distance $m(t_{go})$, generated by an optimal maneuvering target, can be obtained using the adjoint method presented in the previous section. Sufficient conditions for the finite time stability of the guidance loop have been obtained in [5]. In this respect, finite time stability means that a certain quadratic form of the system states, decreases with time. The motivation to associate stability with the guidance loop is based on the “underlying assumption that there exist a strong relation between system stability and miss distance.” Unfortunately, such a stability is not preserved for the entire time interval. However, since in the previous section an explicit function has been presented for the miss distance, the finite time stability becomes redundant. On the other hand, in order to get the *worst* miss distance m^* for any flight time, the function $m(t_{go})$ has to converge to a certain steady-state value. In case there is not a steady-state value, the target is able to obtain any miss distance it desires by maneuvering far enough from collision. Therefore, we seek sufficient conditions for stability of the adjoint guidance loop over the infinite time interval. While in [5] the analysis was implemented in the forward loop, here the adjoint loop is being used. In particular, we are interested in the behavior of $\phi_2(t_{go})$ of Fig. 4, since $m(t_{go})$ is an integral of the absolute value of this signal. To avoid the divergence of $m(t_{go})$ as $t_{go} \rightarrow \infty$ it is necessary that $\phi_2(t_{go})$ converges to zero.

Consider the system described in Fig. 4c, where the signal $\tilde{\phi}_1(t_{go})$ is obtained by

$$\frac{d\tilde{\phi}_1}{dt_{go}} = -\frac{N'}{t_{go}} \mathcal{L}^{-1}\{G_M(s)\tilde{\phi}_1(s)\}, \quad \phi_1(0) = 1 \quad (10)$$

where $\mathcal{L}^{-1}\{\cdot\}$ is the inverse Laplace transform in terms of t_{go} . Using the identity

Fig. 5 The function $m(t_{go})$.

$$\mathcal{L}\{t_{go}f(t_{go})\} = -\frac{df(s)}{ds}$$

we get

$$\mathcal{L}\left\{t_{go} \cdot \frac{df}{dt_{go}}\right\} = -f(s) - s \frac{df(s)}{ds}$$

and Eq. (10) can be rewritten as

$$\frac{d\tilde{\phi}_1(s)}{ds} = \frac{N'G_M(s) - 1}{s} \tilde{\phi}_1(s)$$

Substituting the relation $\tilde{\phi}_1(s) = s\phi_2(s)$ we get

$$\frac{d\phi_2(s)}{ds} = \frac{N'G_M(s) - 2}{s} \phi_2(s) \quad (11)$$

Then, by the inverse Laplace transform,

$$\phi_2(t_{go}) = -\frac{1}{t_{go}} \mathcal{L}^{-1}\{H(s)\phi_2(s)\} \quad (12)$$

where

$$H(s) := \frac{N'G_M(s) - 2}{s} \quad (13)$$

The last result is described in the block diagram of Fig. 6. Note that this is the adjoint for the system described in Fig. 6. Using the block diagram of Fig. 6 is convenient for stability analysis, which we are interested in. Note, however, that this diagram does not contain the same initial condition as in Fig. 4, since during the transformation to the Laplace domain and the elimination of ϕ_1 from the loop, the initial condition has been lost. Instead, any initial condition on the integrator of $H(s)$ will be used as the loop driving force. This can be demonstrated by referring again to Eq. (11), and replacing the right hand side with $d/ds[\phi_2(s) - c]$. By operating the inverse Laplace transform one obtains

$$\phi_2(t_{go}) = c\delta(t_{go}) - \frac{1}{t_{go}} \mathcal{L}^{-1}\{H(s)\phi_2(s)\}$$

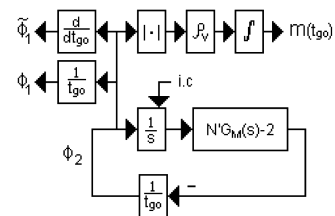


Fig. 6 Block diagram for stability analysis.

where the impulse $\delta(t_{go})$ is the driving force of the system instead of the initial condition on the integrator of $H(s)$, and c is an arbitrary constant. The reader can verify that a specific initial condition will give the actual signals of $\tilde{\phi}_1$, ϕ_1 and ϕ_2 that would arise from the original systems of Fig. 4. Thus, with this specific initial condition we can get all of those signals in one diagram.

The system described in Fig. 6 is linear time variant. Its only time variant element is the feedback gain $1/t_{go}$. In the case of linear time invariant systems, asymptotic stability and bounded input bounded output (BIBO) stability are the same. In the light of Eq. (12), for m^* to be finite we need to make sure that $\phi_2(t_{go}) \rightarrow 0$ as $t_{go} \rightarrow \infty$ exponentially, and as in BIBO stability, we have to make sure that $\phi_2(t_{go})$ does not experience a finite escape time.

From now on we will assume a strictly proper $G_M(s)$, which is reasonable due to the servo of the missile. Hence,

$$H(s)t_{go} = \frac{N'\hat{c}(sI - \hat{A})^{-1}\hat{b} - 2}{s}$$

We adopt a few mathematical properties used in [5,10].

Fact. For any row vector c , a scalar s , and a matrix A (of proper dimensions),

$$sc(sI - A)^{-1} = cA(sI - A)^{-1} + c \quad (14)$$

Proof. $cA(sI - A)^{-1} + c = cA(sI - A)^{-1}[I + (sI - A)A^{-1}] = scA(sI - A)^{-1}A^{-1} = sc[A(sI - A)A^{-1}]^{-1} = sc(sI - A)^{-1}$. \square

Using Eq. (14) with $c = N'\hat{c}\hat{A}^{-1}$ and $A = \hat{A}$ we can write

$$\begin{aligned} N'\hat{c}(sI - \hat{A})^{-1}\hat{b} &= N'\hat{c}\hat{A}^{-1}\hat{A}(sI - \hat{A})^{-1}\hat{b} \\ &= sN'\hat{c}\hat{A}^{-1}(sI - \hat{A})^{-1}\hat{b} - N'\hat{c}\hat{A}^{-1}\hat{b} \end{aligned}$$

In a guidance system we assume that the autopilot is designed for an ideal tracking, which turns out as $G_M(0) = -\hat{c}\hat{A}^{-1}\hat{b} = 1$. Hence,

$$H(s) = N'\hat{c}\hat{A}^{-1}(sI - \hat{A})^{-1}\hat{b} + \frac{N' - 2}{s} \quad (15)$$

A realization for $H(s)$ can be found as

$$\begin{aligned} A_h &:= \begin{bmatrix} \hat{A} & 0 \\ 0 & 0 \end{bmatrix}, & b_h &:= \begin{bmatrix} \hat{b} \\ 1 \end{bmatrix}, \\ c_h &:= [N'\hat{c}\hat{A}^{-1} \quad N' - 2], & d_h &:= 0 \end{aligned} \quad (16)$$

The main result of this Note is the following.

Theorem. Suppose that the following conditions are satisfied: 1) $G_M(s)$ is asymptotically stable; 2) $G_M(s)$ has a unit static gain; 3) $G_M(s)$ is strictly proper; 4) $G_M(s)$ is obtained from a minimal realization; and 5) $N' > 2$. Then, the system described in Fig. 6 is exponentially stable.

Proof. We will separate the proof into three parts: 1) it is shown that there is a solution to the differential equations describing the system in Fig. 6 in the interval $t_{go} \in [0, \infty)$; 2) it will be shown that there is a time interval $[t_{go\min}, \infty)$, where the system is exponentially stable; and 3) finally, by extending the exponential bound for all the entire time interval, it will be concluded that the system is exponentially stable for all $t_{go} \in [0, \infty)$.

Now let us elaborate on these parts.

1) As mentioned previously, it is possible to choose an initial condition for the integrator for Fig. 6 such that $\tilde{\phi}_1(0) = \phi_1(0) = 1$. Thus, $\phi_2(t_{go})$ generated by Fig. 6 is identical to the $\phi_2(t_{go})$ generated by Figs. 4a–4c. In particular, it is convenient to describe $\phi_2(t_{go})$ by Fig. 4c. This system can be described by the state differential equations:

$$\frac{d\tilde{\phi}_1}{dt_{go}} = -\frac{N'}{\theta}(\hat{c}\phi_3 + \hat{a}\phi_1) \quad \phi_1(0) = 1$$

$$\frac{d\phi_2}{dt_{go}} = \phi_1, \quad \phi_2(0) = 0$$

$$\frac{d\phi_3}{dt_{go}} = \hat{A}\phi_3 + \hat{b}\phi_1, \quad \phi_3(0) = 0$$

Rewriting it in a matrix form and assuming $\hat{d} = 0$, we get for $\xi := [\tilde{\phi}_1 \phi_3]'$ the linear differential equation

$$\frac{d\xi}{dt_{go}} = \begin{bmatrix} 0 & -\frac{N'}{t_{go}}\hat{c} \\ \hat{b} & \hat{A} \end{bmatrix} \xi, \quad \xi(0) = \begin{bmatrix} 1 \\ 0 \end{bmatrix} \quad (17)$$

Consider first the interval $[0, \varepsilon]$. Because of the singularity of the adjoint system (17) at $t_{go} = 0$, we say that a solution exists at the origin, if it exists for any arbitrarily small t_{go} . At $t_{go} = 0$, $\xi = [1 \ 0]'$. In addition, at $t_{go} = 0$ we have

$$\begin{aligned} \left. \frac{d\tilde{\phi}_1}{dt_{go}} \right|_{t_{go}=0} &= -\frac{N'}{t_{go}}\hat{c}\phi_3 \Big|_{t_{go}=0} = -\frac{N'\hat{c}\frac{d\phi_3}{dt_{go}}}{1} \Big|_{t_{go}=0} = -N'\hat{c}(\hat{b}\tilde{\phi}_1(0) \\ &+ \hat{A}\phi_3(0)) = -N'\hat{c}\hat{b} \end{aligned}$$

Clearly, this derivative is bounded. Thus, for sufficiently small interval $[0, \varepsilon]$ we can write $\tilde{\phi}_1(\varepsilon) = 1 - N'\hat{c}\hat{b}\varepsilon$. Likewise, $\phi_3(\varepsilon) = \hat{b}\varepsilon$. Next consider the time interval $[\varepsilon, \infty)$. On this interval Eq. (17) is a linear differential equation with continuous coefficients in time. According to Theorem 5.2.1 in [11], this equation has a unique solution. In other words, system (11) has no finite escape time.

2) Let $D(a, b)$ denote a closed disk in the complex plane centered at $-(b+a)/2ab$ with a radius $(b-a)/2ab$, where $0 < a < b$ as described in Fig. 7. Suppose $f(t, y)$ is a nonlinear time varying function, which belongs to the sector $[a, b]$, i.e., $f(t, 0) = 0$, $\forall t \in \mathbb{R}_+$, and $ay \leq f(t, y) \leq by$. According to the circle criterion [10,12] a free system with transfer function $H(s)$, obtained from a minimal realization, and a nonlinear time varying negative feedback $f(t, y)$, which belongs to a sector $[a, b]$, is globally exponentially stable, if the plot of $H(j\omega)$ lies outside and is bounded away from the disk $D(a, b)$. Moreover, the plot encircles $D(a, b)$ exactly r times in the counter-clockwise direction, where r is the number of poles of $H(s)$ with positive real parts. In our case the element $f(t, y)$ is the linear-time-varying function $f(t_{go}) = 1/t_{go}$. According to hypothesis (4) (\hat{A}, \hat{b}) is controllable and (\hat{c}, \hat{A}) observable. Also, hypothesis (5) states that $N' \neq 2$. Hence, by Eq. (16), both the controllability matrix of $H(s)$ and its observability matrix,

$$C = \begin{bmatrix} \hat{b} & \hat{A}\hat{b} \\ 1 & 0 \end{bmatrix}, \quad O = \begin{bmatrix} N'\hat{c} & (N' - 2)\hat{A} \\ N'\hat{c}\hat{A} & 0 \end{bmatrix} \hat{A}^{-1}$$

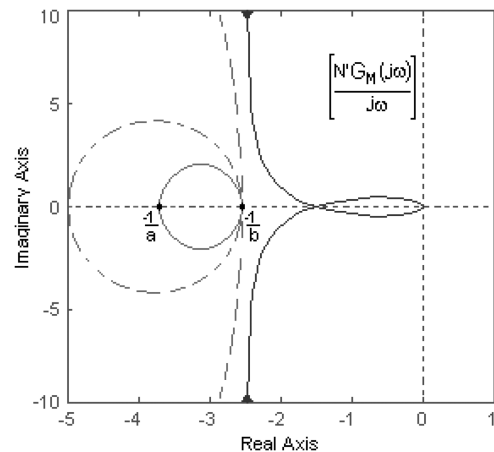


Fig. 7 The circle criterion.

respectively, are of full rank, and the realization of $H(s)$ is minimal. Recall that $H(s)$ is a strictly proper type-one transfer function, and has no poles in the open right half complex plain. In addition, we have the condition $N' > 2$. Thus, $\angle H(j0^+) = -90^\circ$, as can be easily seen by Eq. (16). For type-one systems, the polar plot is completed for the negative values of ω by connecting $H(j0^-)$ to $H(j0^+)$ in the clockwise direction along an infinite radius. Thus, there exists a finite scalar l such that $\operatorname{Re} H(j\omega) > -l$, $\forall \omega \in \mathbb{R}$. Notice that $\operatorname{Re} H(j\omega) = \operatorname{Re}[N'G_M(j\omega)/j\omega]$, so $l = \inf_{\omega \in \mathbb{R}} \operatorname{Re}[N'G_M(j\omega)/j\omega]$. To satisfy the graphical condition in the circle criterion, we place the disc $D(a, b)$ left to the line $\operatorname{Re}[s] = -l$. In particular, choose $l = 1/b$, and let $a \rightarrow 0$, as described in Fig. 7. In the language of the “gain” $1/t_{go}$, the circle criterion is satisfied for the time interval (l, ∞) . Thus, the system in Fig. 6 is exponentially stable in the interval (l, ∞) . This means that there exist constants $k, \lambda > 0$ such that $\|\xi(t_{go})\| \leq k \exp(-\lambda(t_{go} - l))$, $\forall t_{go} \geq l$.

3) Since the solution of the system in Fig. 4c is bounded on the interval $[0, l]$, so does the system of Fig. 6. Thus, there exist a constant $k_1 \geq k$, such that $\|\xi(t_{go})\| \leq k_1 \exp(-\lambda t_{go})$, $\forall t_{go} \in \mathbb{R}_+$. \square

Corollary. Under the conditions of the previous theorem, the miss distance is bounded over the infinite horizon.

Proof. The exponential stability of the $\phi_2(t_{go})$ ensures a finite value for the integral of the absolute value of this signal for all $t_{go} \in \mathbb{R}_+$. Hence, by Eqs. (7) and (8) the worst case miss distance is bounded. \square

V. Conclusions

The miss distance due to a bounded target maneuver against a missile guided by proportional navigation is of great importance. This worst maneuver is bang-bang stairs function. While we do not expect a target to perform the worst possible maneuver, nevertheless, an approximated worst maneuver may induce harmful miss distance. The worst target maneuver changes our view on the miss sensitivity function. One no longer deals with a function approaching zero with time to go as in the case of a step maneuver. Instead, one has a monotonically increasing function representing the miss accumulation with each step maneuver. As indicated in the present Note, under mild conditions, asymptotic stability of the adjoint system is assured, and in turn, implies bounded miss

distance regardless of the flight time. Practically, it means that the worst miss converges in accordance with the missile transfer function poles.

References

- [1] Zarchan, P., *Tactical and Strategic Missile Guidance*, 3rd ed., Vol. 176, Progress in Astronautics and Aeronautics, AIAA, Washington, D.C., 1997.
- [2] Murtaugh, S. A., and Criel, H. E., “Fundamentals of Proportional Navigation,” *IEEE Spectrum*, Vol. A41, Dec. 1966, pp. 75–85.
- [3] Yuan, L., “Homing and Navigational Courses of Automatic Target-Seeking Devices,” *Journal of Applied Physics*, Vol. 19, No. 12, 1948, pp. 1122–1128.
doi:10.1063/1.1715028
- [4] Shinar, J., and Steinberg, D., “Analysis of Optimal Evasive Maneuver Based on a Linearized Two Dimensional Kinematic Model,” *Journal of Aircraft*, Vol. 14, No. 8, Aug. 1977, pp. 795–802.
doi:10.2514/3.58855
- [5] Guelman, M., “The Stability of Proportional Navigation Systems,” *Proceedings of the AIAA, Guidance, Navigation and Control Conference*, 1990, pp. 586–590.
- [6] Gurfil, P., Jodorkovsky, M., and Guelman, M., “Finite Time Stability Approach to Proportional Navigation System Analysis,” *Journal of Guidance, Control, and Dynamics*, Vol. 21, No. 6, Nov.–Dec. 1998, pp. 853–861.
doi:10.2514/2.4348
- [7] Rew, D. Y., Tahk, M. J., and Cho, H., “Short Time Stability of Proportional Navigation Guidance Loop,” *IEEE Transactions on Aerospace and Electronic Systems*, Vol. 32, No. 3, July 1996, pp. 1107–1114.
doi:10.1109/7.532269
- [8] Gutman, S., *Applied Min-Max Approach to Missile Guidance and Control*, Vol. 209 Progress in Astronautics and Aeronautics, AIAA, Washington, D.C., 2005.
- [9] Kailath, T., *Linear Systems*, Prentice–Hall, Upper Saddle River, NJ, 1980.
- [10] Vidyasagar, M., *Nonlinear Systems Analysis*, 2nd ed., Prentice–Hall, Engelwood Cliffs, NJ, 1993.
- [11] Tyn Myint, U., *Ordinary Differential Equations*, Elsevier, New York, 1978, Chap. 5.
- [12] Narendra, K. S., and Taylor, J. H., *Frequency Domain Criteria for Absolute Stability*, Academic Press, New York, 1973.